Hybrid-Mixed Meshless Formulation

J.A. Teixeira de Freitas[1], P.M. Pimenta[2] and S.P.B. Proença[3]

Abstract: *A stress model of the hybrid-mixed formulation is implemented on a compact radial basis and applied to the solution of elliptic problems. The formulation is based on a two-field domain approximation coupled with an independent boundary approximation. It is strictly meshless, as its implementation does not require the decomposition of the domain to define the approximation bases or to support the numerical integration of the coefficients of the solving system. The performance of the formulation is illustrated on a two-dimensional linear elastostatic problem.*

1 Introduction

The meshless formulation used here has been originally developed in the context of the finite element method and applied to the solution of solid mechanics problems. A review of the alternative hybrid-mixed, hybrid and hybrid-Trefftz formulations and their complementary stress and displacement models that have been studied in the context of the finite element method applied to the solution of solid mechanics problems can be found in [1].

The paper reports on the implementation of the stress model of the hybrid mixed formulation in a mesh free context [2]. The formulation used here is termed mixed because two fields are approximated independently in the domain under analysis (the stress and displacement fields). It is termed hybrid because a boundary field is also approximated independently (the boundary displacements in the stress model used here).

This formulation endures two major disadvantages when compared with formulations based on single-field approximations, namely a substantially higher number of degrees-of-freedom and a higher susceptibility to spurious solutions.

The advantages it offers are a better modelling of gradient fields, as they are approximated independently, and the possibility of using virtually any approximation bases, as no constraints are placed a priori in terms of the fundamental equations of the problems.

[1] Instituto Superior Técnico, Universidade Técnica de Lisboa, Lisboa, Portugal (freitas@civil.ist.utl.pt)
[2]Escola Politécnica, Universidade de São Paulo, São Paulo, Brazil (ppimenta@usp.br)
[3] Escola de Engenharia de São Carlos, Universidade de São Paulo, São Carlos, Brazil (persival@sc.usp.br)

In the present context this means that the displacement approximation may not be associated with a compatible strain field and that the stress approximation may not satisfy the equilibrium condition.
This is the feature that is exploited to set up the meshless variant used here. The formulation of the two alternative stress and displacement models is presented in [3], where the definition of the approximation bases and the general expressions of the coefficients of the solving systems can also be found. The associated variational statements and conditions for the existence and uniqueness of the solutions are presented in the same reference. This paper reports on the implementation of the stress model on linear elastostatic problems using compactly supported radial bases [4].

2 Basic equations

In the notation used here, V is the structural domain and Γ its boundary, with complementary parts Γ_σ and Γ_u where forces and displacements are prescribed, respectively.
System (1-5) defines the governing equations for linear elastostatic problems. In the equilibrium and compatibility equations (1) and (2), vectors σ and ε list the independent components of the stress and strain tensors, respectively, and b and u are the body-force and displacement vectors. The differential equilibrium and compatibility operators D and D^* are assumed to be linear and conjugate. In the Neumann and Dirichlet conditions (3) and (4), vectors t_Γ and u_Γ define prescribed forces and displacements. In the constitutive relation (5), f is the flexibility matrix and vectors σ_r and ε_r are used to model residual stress and strain fields, respectively.

$$D\,\sigma + b = 0 \quad \text{in } V \tag{1}$$

$$\varepsilon = D^*\,u \quad \text{in } V \tag{2}$$

$$N\,\sigma = t_\Gamma \quad \text{on } \Gamma_\sigma \tag{3}$$

$$u = u_\Gamma \quad \text{on } \Gamma_u \tag{4}$$

$$\varepsilon = f\left(\sigma - \sigma_r\right) + \varepsilon_r \quad \text{in } V \tag{5}$$

A piecewise linear approximation is assumed for boundary Γ of domain V, which may not be convex or simply connected. The resulting domain is then decomposed in overlapping sub-domains, $V^j \cap V^k \neq 0$, to establish the supports of the independent radial approximations on the stress and displacement fields. Three complementary parts can be distinguished on boundary Γ^j of support V^j, namely a circular part Γ_i^j interior to domain V and the linear segments that may overlap with the Neumann and Dirichlet boundaries, $\Gamma_\sigma^j = \Gamma_\sigma \cap \Gamma^j$ and $\Gamma_u^j = \Gamma_u \cap \Gamma^j$:

$$\Gamma^j = \Gamma_\sigma^j \cup \Gamma_u^j \cup \Gamma_i^j \tag{6}$$

As it is stated below, in the stress model of the hybrid-mixed formulation the displacements are also approximated, and independently, on boundary $\Gamma_\sigma^j \cup \Gamma_i^j$.

4 Stress approximation

The stress field is approximated in each sub-domain V^j in form (7), where matrix S_{Vj} defines the approximation modes, vector X_{Vj} the associated weights and the (optional) particular solution σ_{0j} is used to model local effects, namely those associated with applied domain or boundary loads and with residual stresses:

$$\sigma = S_{Vj}\, X_{Vj} + \sigma_{0j} \quad \text{in } V^j \tag{7}$$

Approximation S_{Vj} is linear independent and defined as follows, where I_σ is the identity matrix with the dimension of the stress field, and r = ρ/R, with R denoting the dimension of the support:

$$S_{Vj} = I_\sigma\, \varphi(r) \tag{8}$$

$$\varphi(r) = (1-r)\, r^n \qquad n = 0, 1, 2, \ldots \tag{9}$$

It is noted that definition (9) includes the radial bases stated in [4]. Therefore, this approximation is not extracted from the solution set of the homogeneous equilibrium equation (1), as it is typical of equilibrium formulations, but satisfies the homogeneous boundary condition (11):

$$D\, S_{Vj} \neq O \quad \text{in } V^j \tag{10}$$

$$N\, S_{Vj} = O \quad \text{on } \Gamma_i^j \tag{11}$$

The conditions above do not apply to the particular solution term, σ_{0j}, which may include non-radial terms, either self-equilibrated or in equilibrium with body forces or with other applied forces.

In order to ensure the invariance of the inner product in the stress mapping, the dual of approximation (7) is used to define the generalised strains (12) and enforce thus in a weak (Galerkin) form the compatibility and elasticity conditions (2) and (5):

$$e_{Vj} = \int S_{Vj}^t\, \varepsilon\, dV^j \tag{12}$$

$$e_{Vj} = \int S_{Vj}^t \left(D^*\, u\right) dV^j \tag{13}$$

$$e_{Vj} = \int S_{Vj}^t \left[f\left(\sigma - \sigma_r\right) + \varepsilon_r \right] dV^j \tag{14}$$

Equation (13) is integrated by parts to establish a single statement on the (weak) enforcement of the kinematic admissibility conditions (2) and (4):

$$e_{Vj} = -\int \left(D\, S_{Vj}\right)^t u\, dV^j + \int \left(N\, S_{Vj}\right)^t u\, d\Gamma_i^j + \int \left(N\, S_{Vj}\right)^t u\, d\Gamma_\sigma^j + e_{\Gamma j} \tag{15}$$

$$e_{\Gamma j} = \int \left(N\, S_{Vj}\right)^t u_\Gamma\, d\Gamma_u^j \tag{16}$$

5 Displacement approximation

Equation (15) together with results (10) and (11) shows that it is necessary to approximate the displacements in the domain of each support V^j and on its Neumann boundary, but that no approximation needs to be enforced on the interior radial boundary Γ_i^j:

$$u = U_{Vj}\, q_{Vj} + u_{0j} \quad \text{in } V^j \tag{17}$$

$$u = U_{\Gamma j}\, q_{\Gamma j} \quad \text{on } \Gamma_\sigma^j \tag{18}$$

As for the stress field approximation, the particular solution u_{0j} is optional and the columns of matrices U_{Vj} and $U_{\Gamma j}$ define the displacement approximation modes in the domain and on the Neumann boundary, with vectors q_{Vj} and $q_{\Gamma j}$ collecting the associated weights. Although this is not strictly necessary [3], compactly supported radial bases are used also to implement approximations (17) and (18):

$$U_{Vj} = I_u\, \varphi(r) \tag{19}$$

$$U_{\Gamma j} = I_u\, \varphi(r) \tag{20}$$

The generalised body and surface forces are defined by their dual transformations (21) and (22) of the displacement approximations, and used to enforce, still in the sense of Galerkin, the static admissibility conditions (1) and (3) for the assumed stress field (7), as stated by equations (23) and (24):

$$Q_{Vj} = \int U_{Vj}^{t}\, b \, dV^{j} \tag{21}$$

$$Q_{\Gamma j} = \int U_{\Gamma j}^{t}\, t_{\Gamma} \, d\Gamma_{\sigma}^{j} \tag{22}$$

$$\int U_{Vj}^{t} \left(D\,\sigma + b \right) dV^{j} = 0 \tag{23}$$

$$\int U_{\Gamma j}^{t} \left(N\,\sigma - t_{\Gamma} \right) d\Gamma_{\sigma}^{j} = 0 \tag{24}$$

6 Displacement approximation

The weak description of the static admissibility condition is obtained enforcing approximation (7) in equations (23) and (24) and recalling definitions (21) and (22):

$$\begin{bmatrix} -A_{Vj}^{t} \\ A_{\Gamma j}^{t} \end{bmatrix} X_{Vj} = \begin{Bmatrix} Q_{Vj} + Q_{V0j} \\ Q_{\Gamma j} - Q_{\Gamma 0 j} \end{Bmatrix} \tag{25a}$$

(25b)

$$A_{Vj} = \int \left(D S_{Vj} \right)^{t} U_{Vj} \, dV^{j} \tag{26}$$

$$A_{\Gamma j} = \int \left(N S_{Vj} \right)^{t} U_{\Gamma j} \, d\Gamma_{\sigma}^{j} \tag{27}$$

$$Q_{V0j} = \int U_{Vj}^{t}\, D\, \sigma_{0j} \, dV^{j} \tag{28}$$

$$Q_{\Gamma 0 j} = \int U_{Vj}^{t}\, N\, \sigma_{0j} \, d\Gamma_{\sigma}^{j} \tag{29}$$

Similarly, the weak description (30) of the kinematic admissibility condition is obtained enforcing the displacement approximations (17) and (18) in equation (15) and using results (26) and (27):

$$e_{Vj} = \begin{bmatrix} -A_{Vj} & A_{\Gamma j} \end{bmatrix} \begin{Bmatrix} q_{Vj} \\ q_{\Gamma j} \end{Bmatrix} + e_{\Gamma j} - e_{V0j} \tag{30}$$

$$e_{V0j} = \int \left(D S_{Vj} \right)^{t} u_{0j} \, d\Gamma^{j} \tag{31}$$

The static and kinematic admissibility conditions (25) and (30) are dual and independent of the constitutive relations. In the present context, these relations are established enforcing the stress approximation (7) in the weak form (14):

$$e_{Vj} = F_{Vj}\, X_{Vj} + e_{E0j} \tag{32}$$

$$F_{Vj} = \int S_{Vj}^{t}\, f\, S_{Vj} \, dV^{j} \tag{33}$$

$$e_{E0j} = \int S_{Vj}^{t} \left[f \left(\sigma_{0j} - \sigma_{r} \right) + \varepsilon_{r} \right] dV^{j} \tag{34}$$

The solving system is obtained combining equations (25), (30) and (32), to eliminate the generalised strains as independent variables:

$$\begin{bmatrix} F_{V} & A_{V} & -A_{V} \\ A_{V}^{t} & \circ & \circ \\ -A_{\Gamma}^{t} & \circ & \circ \end{bmatrix}_{j} \begin{Bmatrix} X_{V} \\ q_{V} \\ q_{\Gamma} \end{Bmatrix}_{j} = \begin{Bmatrix} e_{\Gamma} - e_{V0} - e_{E0} \\ -Q_{V0} - Q_{V} \\ Q_{\Gamma 0} - Q_{\Gamma} \end{Bmatrix}_{j} \tag{35}$$

The solving system for domain V presents the same sparse structure, and features symmetry whenever the same property holds for the local flexibility matrix, f. According to definitions (7) and (17), vectors X_{Vj} and q_{Vj} are strictly dependent on

support V^j and definitions (6) and (18) show that the generalised boundary displacements $q_{\Gamma j}$ are the only shared variables. However, they are shared only by supports containing the same portions of Neumann boundary Γ_σ.
Consequently, the solving system is particularly well suited for parallel processing and should be processed exploiting its sparsity fully. The flexibility matrix F_V is block-diagonal and the coefficients of matrices A_V and A_Γ are determined by direct allocation of the contribution of each support.
Besides being instrumental to model local effects, the particular terms present in the domain approximations (7) and (17) can be used also to simplify the calculation of the stipulation vector of the solving system (35), for instance by avoiding the calculation of domain integral terms. It can be easily confirmed that condition (11) and definitions (36) and (37) ensure results (38) and (39), provided that σ_b and u_b define a particular solution for the body force field, σ_r is a (self-equilibrated) residual stress field and u_b is a displacement field compatible with the residual strain field, ε_b:

$$\sigma_{0j} = \sigma_b + \sigma_r \tag{36}$$

$$u_{0j} = u_b + u_r \tag{37}$$

$$e_{V0j} + e_{E0j} = \int \left(N S_{Vj}\right)^t u_{0j}\, d\Gamma_u^j + \int \left(N S_{Vj}\right)^t u_{0j}\, d\Gamma_\sigma^j \tag{38}$$

$$Q_{V0j} + Q_{Vj} = 0 \tag{39}$$

7 Numerical implementation and testing

A detailed description and assessment of the implementation of the solving system (35) for compactly supported radial bases can be found in [2], from where the test results presented below on the quadrant of a doubly-symmetric cracked plate shown in figure 1 are taken.

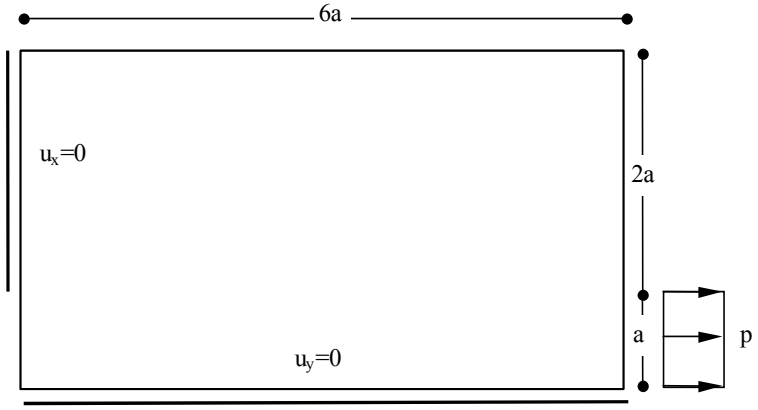

Figure 1: *Cracked plate under tension.*

These results are obtained with a regular grid of $M = m_x \times m_y$ points, the origins of the compact supports with constant radius R, to yield $M = (6a/R+1)\times(3a/R+1)$ for this particular test. The dimensions of the stress basis $N_\sigma = 3M\times(n_\sigma+1)$ and the dimensions of the domain and boundary displacement approximations bases are $N_u = 2M\times(n_u+1)$ and $N_\Gamma = (28a/R-2)\times(n_\Gamma+1)$, respectively, where n_σ, n_u and n_Γ define the order used in each approximation. Each support interacts with eight domain supports and two boundary supports, at the most. Consequently, the sparsity indices are very high, well above 99.9% for systems with dimension $N > 10^4$.

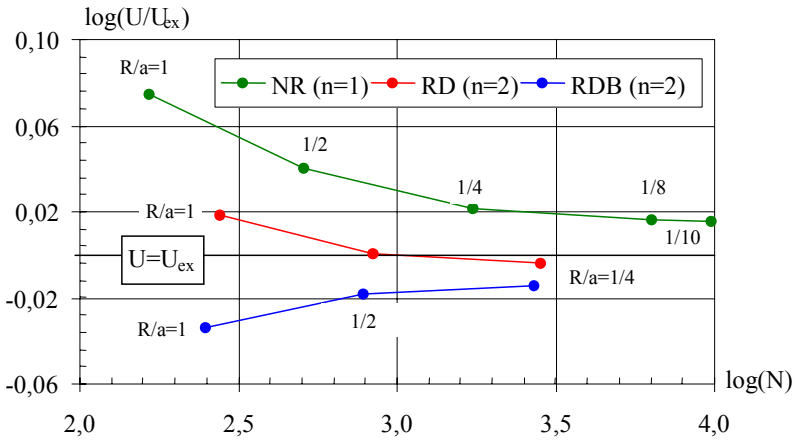

Figure 2: *Convergence in energy under h-refinement.*

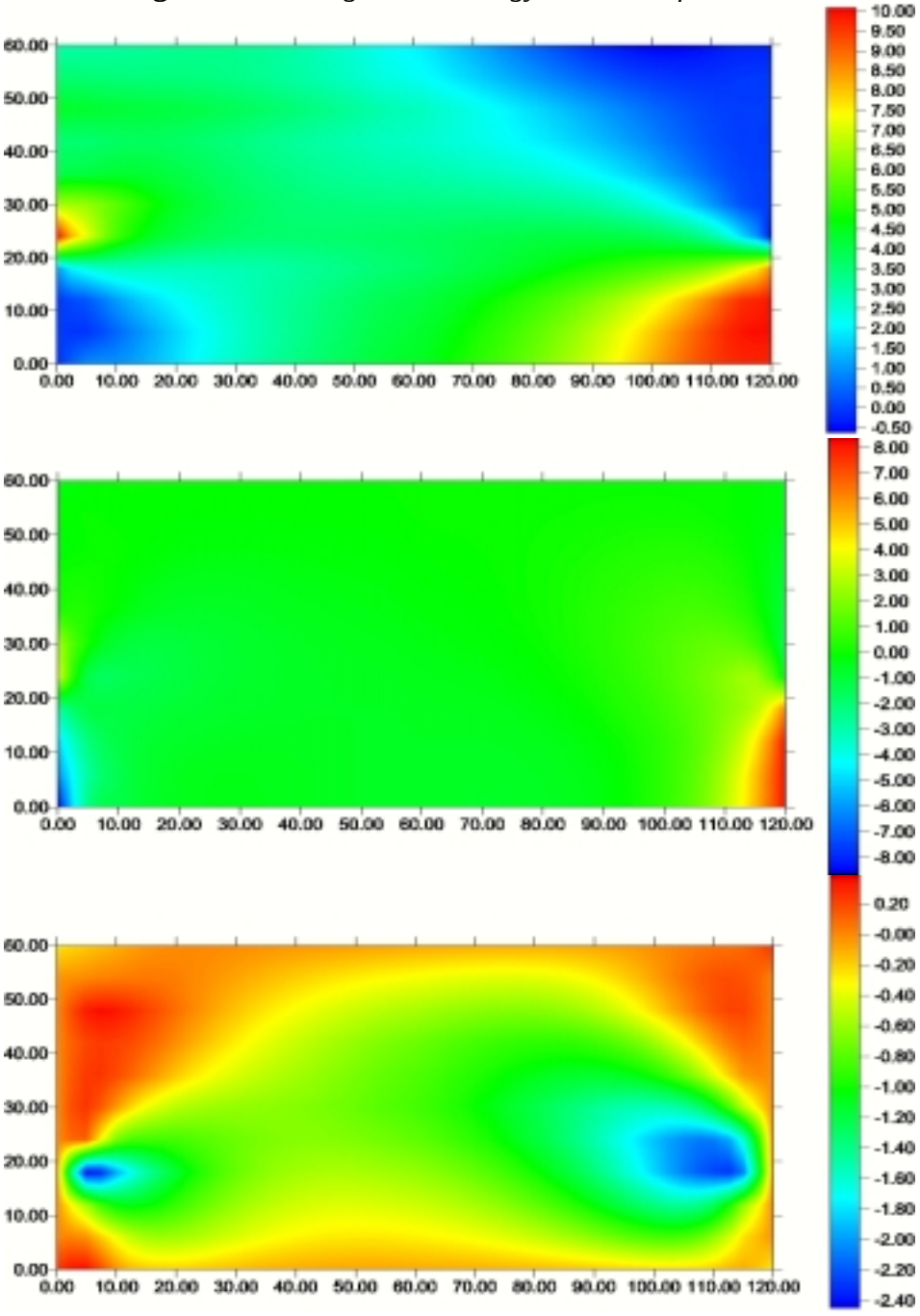

Figure 3: *Estimates for the stress components (σ_{xx}, σ_{yy}, σ_{xy}).*

The h-refinement convergence patterns in energy are shown in figure 2 for different bases, namely a non-relaxed basis (NR), with $n_\sigma = n_u = n_\Gamma = n = 1$, and two bases designed to relax the enforcement of the equilibrium condition in the domain (RD) and on the boundary (RDB), with $n_\sigma = n_u + 1 = n_\Gamma = n$ and $n_\sigma = n_u + 1 = n_\Gamma + 1 = n$, respectively. The reference value for the strain energy is $U_{ex} \approx 0{,}0458403\ (6pa)^2/E$, where E is the modulus of elasticity of the plate.
The patterns shown in figure 2 recover those reported in [1] for the finite element version of the stress model of the hybrid-mixed formulation used here, implemented on polynomial bases relaxed in the domain and on the boundary. The higher convergence rates shown there under p-refinement result from the completeness of the bases used.
The stress estimates shown in figure 3 are obtained for refinement R/a=1/8 and the same degree in all approximation bases ($n_\sigma = n_u = n_\Gamma = 0$). This simulation involves a total 6347 degrees-of-freedom, with 3675 stress modes, 2450 displacement modes in the domain and 222 boundary displacement modes.
The illustrations show that the boundary conditions are enforced adequately. However, the discontinuity of the stress field and the applied load and, in particular, the stress singularity at the crack tip are not modelled with the expected level of accuracy. This is due to the relatively coarseness of the mesh being used (R = 2.5 for a = 20) with regard to the high gradients expected, which cannot be captured with the stress interpolation from the grid points used to obtain the illustrations in figure 3. Moreover, it is enhanced by the weak and incomplete nature of the radial basis applied in the tests.

8 Closure

The meshless version of the hybrid-mixed formulation reported here shares the symmetry, high sparsity and suitability for parallel processing already reported for the finite element variant. It enjoys the added advantage of involving a boundary basis smaller in dimension, as a result of the radial basis property (11), which does not hold for finite element bases, and it is, in consequence, less susceptible to spurious solutions.
The major weakness of the meshless implementation reported here is the use of incomplete bases, which prevents the proper use of p-refinement, responsible for substantially higher rates of convergence. This limitation can be overcome by enriching and refining the bases locally, namely through the use partition of unity bases.

Acknowledgement: This research is part of the bilateral co-operation project 75/01 supported by GRICES, Portugal, and CAPES, Brazil.

References

[1] J.A.T. Freitas, J.P.M. Almeida, E.M.B.R. Pereira, "Non-conventional formulations for the finite element method", *Comput. Mech.*, **23**, 5-6, 488-501 (1999).
[2] J.A.T. Freitas, P.M. Pimenta, S.P.B. Proença, "Formulação híbrida-mista de tensão sem malha com base compacta de funções radiais", *in Métodos Numéricos en Ingeniería V*, J. M. Goicolea, C. Mota Soares, M. Pastor y G. Bugeda (Eds.), SEMNI, Spain, 2002
[3] J.A.T. Freitas, "Hybrid-mixed meshless formulation with compactly supported radial basis: development, implementation and theory", Rel. Int., ICIST, 2001.
[4] H. Wendland, "Piecewise polynomial, positive definite and compactly supported radial basis functions of minimal degree", *Adv. Comput. Math.*, **4**, 389-396 (1995).